RSC Advances

ROYAL SOCIETY OF CHEMISTRY

www.rsc.org/advances

Use multi-particle delivery system to increase the bioavailability of tangeretin.

1   **Improving nutraceutical bioavailability using mixed colloidal delivery**

2   **systems: Lipid nanoparticles increase tangeretin bioaccessibility and**

3   **absorption from tangeretin-loaded zein nanoparticles**

4   **Jingjing Chen[1], Jinkai Zheng[1,2], Eric A. Decker[1], David Julian McClements[1,3+],**

5   **Hang Xiao[1+]***

6   [1] Department of Food Science, University of Massachusetts, Amherst, MA 01003, USA

7   [2] Institute of Agro-Products Processing Science and Technology, Chinese Academy of

8   Agricultural Sciences, Beijing, China

9   [3] Department of Biochemistry, Faculty of Science, King Abdulaziz University, P. O. Box 80203,

10   Jeddah 21589, Saudi Arabia

11

12

13

14

15

16

17

18   *** Contact Details:** Department of Food Science, University of Massachusetts, Amherst, MA

19   01003, USA; email: hangxiao@foodsci.umass.edu; Tel: 413 545 1023

20   + These authors contributed equally to this manuscript.

21

22

Abstract

The objective of this study was to evaluate the influence of dietary lipids on the gastrointestinal fate of tangeretin-loaded zein nanoparticles. The zein delivery systems were mixed with different amounts of oil-in-water emulsions to represent varying levels of digestible fat in the diet, and then passed through a simulated gastrointestinal tract model. Tangeretin bioaccessibility increased with increasing fat content due to enhanced solubilization within the mixed micelles formed by lipid digestion products (fatty acids and monoacylglycerols) in the intestinal fluids. Indeed, the tangeretin concentration in the micelle phase was about twelve times higher in the presence of fat droplets than in their absence. The intestinal epithelium absorption study indicated that tangeretin permeability across the model epithelium cells also increased with increasing fat content. This study suggests that utilizing mixed colloidal systems consisting of both lipid nanoparticles and protein nanoparticles may promote the bioavailability of hydrophobic bioactive agents.

1. Introduction

Tangeretin represents a class of polymethoxy flavonoids (PMFs) found almost exclusively in citrus fruits, and particularly the peels of sweet and mandarin oranges [1]. PMFs have been shown to exhibit a variety of potential benefits for human health, such as enhancing biochemical events in mammalian cells [2], reducing serum triacylglycerol, very low-density lipoprotein (VLDL), and low-density lipoprotein (LDL) levels [3]. PMFs can also inhibit the proliferation of certain types of cancer cells, such as lung, colon and breast cancer cells [4]. PMFs have also been demonstrated to modulate the liver and heart function of hypercholesterolemic of rats [5].

However the oral bioavailability of tangeretin is currently limited due to its poor water solubility, which is related to the presence of numerous methoxyl groups on the flavone backbone [6]. We have previously shown that zein nanoparticles and microparticles offer a suitable means of encapsulating and delivering tangeretin [7]. Colloidal particles can be formed from zein using antisolvent precipitation due to its high solubility in alcohol solutions but low solubility in water [8]. The zein and active component are dissolved in an alcohol solution, which is then injected into water, resulting in the spontaneous formation of zein particles containing the active component. This method has been successfully used to encapsulate lipids, such as fish oil, flax oil, and essential oils [9].

The purpose of the current study was to examine the impact of lipid nanoparticles on the potential gastrointestinal fate of tangeretin-loaded zein nanoparticles. It is well known that co-ingestion of digestible lipids can increase the oral bioavailability of lipophilic nutraceuticals and pharmaceuticals by altering their bioaccessibility, absorption, or transformation within the gastrointestinal tract [10]. Lipids may enhance the bioavailability of lipophilic molecules through a variety of mechanisms, including stimulating the secretion of digestive juices, increasing gastrointestinal transit times, enhancing their solubility within intestinal fluids through mixed micelle formation, increasing the permeability of the epithelium monolayer, controlling chemical or biochemical transformation, or altering the absorption route (portal vein *versus* lymphatic system). Recent study showed that the bioefficacy of tangeretin against cancer cells were significantly improved when they were administered in emulsion [11]. Both in vitro and in vivo studies indicated the bioavailability of tanteretin was increased when incorporated in to lipid nanoemulsion[12]. We therefore hypothesized that mixing tangeretin-loaded zein nanoparticles

75   with digestible lipid nanoparticles would enhance the bioavailability of the lipophilic tangeretin

76   molecules. The influence of lipids on the potential biological fate of the tangeretin was studied

77   using a simulated gastrointestinal model that included mouth, stomach, and small intestine

78   phases, combined with a Caco-2 cell model to study permeability [6].

79   An important aim of this study was to highlight the potential advantages of using

80   combination delivery systems containing a mixture of different types of colloidal particles (in

81   this case zein and lipid nanoparticles) rather than using single types of colloidal particle. This

82   information may be useful in the rational design of oral delivery systems for food and

83   pharmaceutical applications.

84   ## 2. Materials and Methods

85   ### 2.1. Materials

86   Tangeretin powder with a purity of 98.4% was obtained from Bepharm Ltd. (Shanghai,

87   China). β-lactoglobulin (with a purity of 92.5%) was obtained from Daviso Foods International

88   (lot JE 002-8-415, Le Sueur, MN). Corn oil was obtained from a local supermarket. Zein (purity

89   92%, w/w), bile extract (porcine, B8613), porcine pancreas (Type II, triacylglycerol hydrolase

90   E.C. 3.1.1.1, PPL), Hank's balance salts (cat. no. H1387) and uranyl acetate were purchased from

91   Sigma-Aldrich (St Louis, MO). Pepsin (CAS: 9001-75-6), sodium chloride (NaCl), sodium

92   hydroxide (NaOH), calcium chloride ($CaCl_2$), hydrochloric acid (HCl), HPLC grade methanol,

93   tetrahydrofuran (THF), trifluoroacetic acid (TFA), acetonitrile (ACN) were obtained from Fisher

94   Scientific (Fairlawn, NJ, USA). Ammonium acetate was obtained from EMD Chemicals Inc.

95   (Gibbstwon, NJ, USA). Double distilled water was made from a water purification system

96   (Model D14031, Barnstead Nanopure water system, Dubuque, Iowa, USA). DMEM (Dulbecco's

97   Modification of Eagle's Medium) and non-essential amino acid was purchased from Mediatech

98   Inc., (Manassas, VA). HEPES was purchased from Acros Organics (Geel, Belgium).

99   ### 2.2. Preparation of tangeretin-loaded zein nanoparticles

100   The tangeretin-loaded zein nanoparticles were made using an antisolvent precipitation

101   method described previously [13], with some slight modifications. The particles were prepared by

102   injecting an organic phase into an aqueous phase. The organic phase consisted of zein and

103   tangeretin (25:1, w/w) dissolved in 90% ethanol solution, while the aqueous phase consisted of

104   β-lactoglobulin (3%, w/v) dissolved in PBS (10 mM, pH 7). The zein nanoparticles were formed

105   spontaneously when the organic phase was injected into the aqueous phase (1:3, v/v) dropwise

106   under constant stirring at 1000 rpm (Corning Stirrer PC-420, Corning Inc., USA). The ethanol in

107   the mixture was then evaporated with using a vacuum rotary evaporator (Rotavapor R110, Buchi

108   Crop., Switzerland). Then the sample was freeze dried (VirTis Genesis Lyophilizer, Virtis

109   genesis company inc., USA) and kept in a refrigerator prior to further use.

110   **2.3. Preparation of lipid nanoparticles**

111   β-lactoglobulin was dissolved in 10 mM phosphate buffer (3%, w/w) and stirred for at least

112   2 hours to ensure full hydration. A coarse emulsion was prepared by mixing 20% corn oil with

113   aqueous solution using a hand blender (M133/1280, Biospec Products, Inc., ESGC, Switzerland)

114   for 2 min. This coarse emulsion was then passed through a high pressure homogenizer

115   (Microfluidics M-110Y, Newton, MA) at 12,000 psi for 3 times.

116   **2.4. Particle size and ζ-potential measurement**

117   The particle size and ζ-potential of the nanoparticles were determined using a commercial

118   dynamic light scattering and micro-electrophoresis device (Nano-ZS, Malvern Instruments,

119   Worcestershire, UK). The samples were diluted 10 times in PBS buffer solutions (pH 7) at the

120   same pH as the samples being analyzed at room temperature before measurement. The particle

121   size is reported as the intensity-weighted ('Z-average') mean particle diameter, while the particle

122   charge is reported as the ζ-potential.

123   **2.5. Microstructure & visual observations**

124   The microstructure of the colloidal delivery systems was observed using an optical

125   microscope (Nikon Eclipse E400, Nikon Corp., Japan), and the resulting images were acquired

126   using digital image processing software (Micro Video Instruments Inc., Avon, MA). Selected

127   samples were also analyzed using transmission electron microscopy (JEOL JEM-2000FX, JEOL

128   USA, Inc., MA, USA). The general appearance of the colloidal systems and digesta after

129   different gastrointestinal stages were recorded by taking images using a digital camera

130   (Powershot SD1300IS, Canon).

2.6. Potential gastrointestinal fate of tangeretin-loaded zein nanoparticles

An *in vitro* digestion model was used to study the potential behavior of the delivery systems under simulated gastrointestinal tract [14] conditions. Experiments were carried out at different lipid contents by mixing the tangeretin-loaded zein nanoparticles with lipid nanoparticles to simulate different diet compositions (*i.e.* high *versus* low fat diets).

Different delivery systems were prepared by mixing the freshly prepared tangeretin-loaded zein nanoparticles and different amounts of stock nanoemulsion and phosphate buffer solution so that they differed only in oil content (0%, 2%, and 4%). The samples were then passed through a simulated GIT similar to that described earlier [15], but with some slight modifications.

Mouth phase: Oral conditions were mimicked by mixing the delivery systems with a simulated saliva fluid (SSF), which was prepared from various salts and mucin as described previously [16]. Delivery systems were mixed with SSF at a 1:1 volume ratio, and then the resulting mixture was adjusted to pH 6.8 and shaken continuously at 100 rev/min in an incubator at 37 ºC for 10 min (Innova Incubator Shaker, Model 4080, New Brunswick Scientific, New Jersey, USA).

Stomach phase: Simulated gastric fluid was prepared by mixing 2 g of NaCl and 7 ml of concentrated HCl and then making the volume up to 1 L using distilled water [16]. Pepsin was then dissolved in this mixture (0.32 %, w/v), the pH was adjusted to 1.2, and the sample from the mouth phase was mixed with it at a 1:1 volume ration. The resulting mixture was then adjusted to pH 2.5 and incubated at 100 rev/min and 37 ºC for 2 hr.

Small intestine: Small intestine conditions were simulated using a pH-stat automatic titration unit (Metrohm, USA Inc.). The sample collected from the stomach phase was placed in a container placed in a 37 ºC water bath. The pH was adjusted to pH 7.0. Bile salt (187.5 mg in 4 ml pH 7 PBS buffer solution) was then added, and the pH was adjusted back to 7.0. Calcium chloride solution (110 mg dissolved in 1 ml double distilled water) was then added and again the pH was adjusted to 7.0. Finally, freshly prepared pancreatin lipase (60 mg lipase in 2.5 ml pH 7.0 PBS) was added to the solution. At the same time, the automatic titration of pH-stat was started. The free fatty acid released during digestion was calculated using the following equation [17]:

$$FFA\% = 100 \times \left(\frac{V_{NaOH} \times m_{NaOH} \times M_{lipid}}{w_{lipid} \times 2} \right) \tag{1}$$

160   Here, V_{NaOH} is the volume of sodium hydroxide solution required to neutralize the free fatty

161   acids (and other sources of H^+) released during digestion; m_{NaOH} is the molar concentration of

162   sodium hydroxide solution, which is 0.25 M in this study; M_{lipid} is the molecular weight of corn

163   oil, which is 800 g/mol; w_{lipid} is the amount of oil in the reaction system.

164   **2.7. Bioaccessibility determination**

165   The samples obtained after *in vitro* digestion were collected and centrifuged (Centrifuge

166   5417R, Eppendorf co., Hamburg, Germany) (20200 g, 14000 rpm) at 4 ºC for 40 min. The clear

167   micelle phase on the top layer of the samples was filtered through a 220 nm syringe filter (EMD

168   Millipore, Billerica, MA) and analyzed for the tangeretin content using the HPLC method

169   described before [18]. The bioaccessibility was then calculated using the following equation:

170    $$Bioaccessibility(\%) = \frac{C_{Micelle}}{C_{RawDigesta}} \times 100\% \qquad (2)$$

171   Here, $C_{Micelle}$ is the concentration of tangeretin in the filtered micelle phase, and $C_{Raw\ Digesta}$ is the

172   concentration of tangeretin in the raw digesta.

173   **2.8. Cytotoxicity measurement of micelle phase**

174   Caco-2 cells were seeded in 96-well plates at a density of 20,000 cells/well in 200 μL

175   complete DMEM media (10% FBS, 1% antibiotic, 1% non-essential amino acid). After 24 h,

176   cells were treated with different concentrations of micelle phase diluted with serum complete

177   media. Tangeretin dissolved in DMSO was used as a control group and the final DMSO

178   concentration in the medium was less than 1%. After incubation for 24 h, cells were analyzed

179   using the 3-(4,5-dimethylthiazol-2-yl)-2,5-diphenyltetrazolium bromide (MTT) assay. Media in

180   each well was replaced by 100 μL freshly prepared MTT solution (0.5 mg/mL dissolved in

181   DMEM media). After 2 h incubation at 37 ºC, MTT solution was dumped and the reduced

182   formazan dye was solubilized by adding 100 μL of DMSO to each well. After gentle mixing, the

183   absorbance was monitored at 570 nm using a plate reader (TECAN, Phenix Research Products,

184   Candler, NC, USA) [19].

7

185 **2.9. Tangeretin permeability determination using Caco-2 monolayers**

186   Caco-2 cell monolayer maintenance and permeability determination was conducted as

187 described before [20]. Caco-2 cells were seeded on transwell permeable supports containing 0.4 μm

188 polycarbonate membranes (Corning Incorporated, Corning, NY) at a seeding density of 2.6×10^5

189 cells / cm^2. The medium was changed 16 h after seeding. The media in the apical and basolateral

190 compartments were changed every other day. This process was maintained for about 21 days

191 until the transendothelial electrical resistance of the filter was about 260 Ω cm^2.

192   The micelle phases were collected after *in vitro* digestion and filtered through a 220 nm

193 membrane. They were then diluted with Hank's Balanced Salt (HBSS, pH 7.4) to obtain

194 tangeretin concentrations suitable for permeability determinations. Tangeretin dissolved in

195 DMSO was used as a control group. All the solutions used in this experiment were pre-warmed

196 in a 37 ºC water bath. The Caco-2 monolayer transwell was incubated with HBSS for 30 min

197 before the experiment. Then both the apical and basolateral compartments were rinsed twice with

198 HBSS). An aliquot (1.5 ml) of each sample was added to the apical compartment and 2.5 ml pre-

199 warmed HBSS was added to the basolateral compartment. Then, this plate was placed in an

200 incubator. Every 30 min, 200 μL of solution was withdrawn from the apical compartment

201 without adding new sample and 100 μL of sample was taken from the basolateral compartment

202 and replaced by same amount of pre-warmed HBSS. The whole experiment duration was 2 hours.

203 The transendothelial electrical resistance were monitored every time before and after the

204 experiment and before each sampling time. The concentration of tangeretin in each sample were

205 analyzed using HPLC method. The apparent permeability coefficient (cm s^{-1}) was calculated

206 with the following equation:

207     $P_{app} = (dQ/dt)(1/(AC_0))$ (3)

208 dQ/dt is the steady-state flux (μmol s^{-1}), A is the surface of the filter (4.67 cm^2), C_0 is the

209 concentration of tangeretin added to apical compartment of each well (μM).

210 **2.10. Data analysis**

211   All data in this study are expressed as mean ± SD. Student's t-test was used to determine the

212 significance of difference between two groups. One way ANOVA was used to analyze the

213 significance of difference for more than three groups. 5% significance level was used for all tests.

3. Results and Discussion

3.1. Characterization of delivery systems

In this study, mixed delivery systems were prepared that contained a combination of tangeretin-loaded zein nanoparticles and digestible lipid nanoparticles. Knowledge of the initial characteristics of these nanoparticles is important to understand their subsequent behavior in the simulated GIT. We therefore measured the size, charge, and morphology of the particles using light scattering, electrophoresis, and microscopy. The mean particle diameters of the freshly prepared nanoemulsions, tangeretin-loaded zein nanoparticles, and their mixture were 197, 248, and 215 nm respectively (**Fig.1**). The ζ-potentials of the initial lipid nanoparticles (- 29 mV), tangeretin-loaded zein nanoparticles (-25 mV) and mixed system (-52 mV) were all highly negative. The transmission electron microscopy (TEM) measurements suggested that the zein nanoparticles (smooth surfaces) and lipid nanoparticles (crinkly surfaces) existed separately in the mixture (**Fig. 1**), which can be attributed to the strong electrostatic repulsion between them. We confirmed the nature of the different kinds of nanoparticles in the mixed systems by taking TEM images of samples containing only lipid nanoparticles which had crinkly surfaces and only zein nanoparticles which had smooth surfaces (data not shown). The crinkly appearance of the lipid nanoparticles is probably due to crystallization of the uranyl acetate dye on their surfaces during sample preparation for electron microscopy. Optical microscopy images of the mixed delivery systems confirmed that they had good stability to aggregation, with no evidence of large particles in the system (**Fig. 2a**). The colloidal delivery systems all had good stability to gravitational separation (creaming or sedimentation), as demonstrated by the fact that no phase separation was observed after 24 hours incubation, which can be attributed to their small initial particle size and stability to aggregation.

3.2. Gastrointestinal fate of colloidal delivery systems

Colloidal delivery systems encounter a series of physicochemical and physiological environments as they pass through the various stages of the human GIT, such as changes in pH, ionic strength, agitation, enzyme activities, and surface active agents [21]. We therefore measured changes in the properties of mixed colloidal delivery systems (containing 2% fat) as they passed through the simulated mouth, stomach, and small intestine phases of the GIT model.

243   *Mouth:* The mean diameter of the particles in the system increased from around 215 to 424
244   nm after incubation in the simulated saliva fluids (**Fig. 3a**), which suggests that some particle
245   aggregation occurred. This observation was supported by the optical microscopy images, which
246   clearly showed evidence of extensive particle aggregation (**Fig. 2b**). The origin of this effect can
247   be attributed to particle flocculation induced by the presence of mucin in the artificial saliva.
248   Mucin is a large glycoprotein that can promote particle aggregation under oral conditions
249   through both bridging and depletion mechanisms [22]. The magnitude of the negative charge on
250   the particles decreased when they moved from the initial to the mouth phases (**Fig. 3b**), which
251   can be attributed to electrostatic screening effects by salts in the simulated saliva, as well as to
252   possible adsorption of mucin molecules to the lipid droplet surfaces.

253   *Stomach:* There was a large increase in the mean particle diameter measured by light
254   scattering (**Fig 3a**) and evidence of extensive particle aggregation in the optical microscopy
255   images (**Fig 2c**) when the samples moved from the mouth to the stomach phases. A number of
256   different physicochemical phenomena may contribute to the instability of the nanoparticles
257   within the gastric environment. First, both the zein and lipid nanoparticles used in this study
258   were coated with a globular protein (β -lactoglobulin) that has an isoelectric point around pH 5.
259   Consequently, the nanoparticles will have passed through a point of zero charge when they
260   moved from the simulated mouth (pH 7) to the simulated gastric (pH 2) fluids, which may have
261   promoted irreversible aggregation due to a reduction in electrostatic repulsion. Second, anionic
262   mucin molecules from the saliva may have caused bridging flocculation of the cationic protein-
263   coated nanoparticles in the stomach. Third, the relatively high ionic strength of the gastric fluids
264   may have reduced any electrostatic repulsion between the nanoparticles leading to aggregation.
265   Fourth, hydrolysis of the β-lactoglobulin coating around the nanoparticles by digestive enzymes
266   (pepsin) may have reduced their aggregation stability. The electrical charge on the nanoparticles
267   in the stomach was close to zero (**Fig. 3b**). One might expect nanoparticles coated by β -
268   lactoglobulin to be strongly positively charged at pH 2 because this is well below their isoelectric
269   point. The fact that the charge was near zero may have been because anionic mucin adsorbed to
270   the droplet surfaces, thereby neutralizing some of the positive charge from the proteins. In
271   addition, some of the surface proteins may have been digested by the pepsin, which would have
272   altered the surface charge. The droplets in the emulsion were highly unstable to gravitational
273   separation (**Fig. 3a**) under gastric conditions, which can be attributed to the relatively large

10

274 particle size caused by droplet aggregation. Interestingly, we did not observe a sediment layer in

275 these systems suggesting that the zein nanoparticles associated with the lipid nanoparticles and

276 the overall density of the flocs formed was less than that of water.

277   *Small Intestine:* The mean particle diameter remained relatively large after incubation in the

278 small intestinal fluids (**Fig. 3a**), but the large aggregates formed within the gastric fluids

279 appeared to have largely dissociated (**Fig 2d**). In the presence of pancreatin, the triacylglycerol

280 molecules in the lipid droplets will be converted to a monoacylglycerol [23] and two free fatty

281 acids (FFAs) by pancreatic lipase. These MAG and FFAs will combine with phospholipids and

282 bile salts to form mixed micelles (micelles and vesicles) that can solubilize lipophilic compounds,

283 and then carry them through the mucous layer to the small intestine cell surfaces [10a]. The

284 pancreatic lipase used in this study was a crude extract that also has protease activity.

285 Consequently, the β -lactoglobulin and zein in the protein nanoparticles would have been fully or

286 partially hydrolyzed, thereby releasing the tangeretin in the intestinal fluids. As a result, the

287 digesta is likely to contain a complex mixture of different types of colloidal particles, including

288 undigested lipid particles, undigested protein particles, micelles, vesicles, and insoluble matter.

289 The high negative charge on the particles in these samples can therefore be attributed to the

290 anionic nature of the free fatty acids, bile salts, phospholipids, and proteins at neutral pH

291 conditions (**Fig. 3b**).

292 **3.3. Digestibility of colloidal delivery systems**

293   In this section, we used the pH-stat method to measure the digestion of the various colloidal

294 delivery systems. As mentioned earlier, the crude pancreatic lipase extract used in this study has

295 both lipase and protease activity, and therefore we would expect both the proteins and lipids to

296 be digested. The amount of alkaline solution required to maintain the solution at pH 7.0

297 throughout the digestion period was measured (**Fig. 4a**), and then this information was used to

298 calculate the percentage of free fatty acids (FFA) released from the samples containing lipid

299 nanoparticles (**Fig. 4b**). Prior to calculating the FFAs for these samples, the volume of alkaline

300 solution titrated into the lipid-free solutions was subtracted to take into account changes in pH

301 induced by protein digestion.

302   The volume of alkaline solution titrated into the samples increased rapidly during the first

303 few minutes of digestion, and then increased more gradually at longer digestion times (**Fig. 4a**).

304   The fact that an appreciable increase in volume was observed for the system containing no lipids

305   can be attributed to the hydrolysis of proteins (β -lactoglobulin and/or zein). For both systems

306   containing lipid nanoparticles, there was a rapid initial increase in FFAs released during the first

307   10 minutes, and then a relatively constant value was reached at longer times (**Fig. 4b**). These

308   results suggest that the lipid phases were fully digested within the small intestine stage, thereby

309   leading to the formation of free fatty acids and monoacylglycerols that could form mixed

310   micelles to solubilize the tangeretin. The fact that the delivery system initially containing 4% oil

311   had twice as much digestible lipid as the one containing 2% oil would be expected to lead to

312   more mixed micelles.

313   **3.4. Tangeretin bioaccessibility**

314   The amount of a lipophilic bioactive component solubilized within the mixed micelle phase

315   is normally taken as a measure of its bioaccessibility [24]. We therefore analyzed the amount of

316   tangeretin in the mixed micelle phase obtained by centrifuging the digested sample collected at

317   the end of the GIT model. Normally after centrifugation, the digested sample has three layers: a

318   creamy layer at the top containing any undigested lipid; a clear layer at the middle containing the

319   mixed micelles; and a pellet at the bottom containing dense insoluble materials, such as calcium

320   soaps, undigested proteins, and precipitated compounds [10a]. In our study, all of the fat in the

321   delivery systems was fully digested (**Fig. 4b**), and so only two layers were observed: the mixed

322   micelle phase and the pellet.

323   The bioaccessibility of the tangeretin increased as the concentration of co-ingested lipid

324   phase increased (**Fig. 5),** being around 15, 26, and 37 % for delivery systems initially containing

325   0, 2 and 4% oil. As mentioned earlier, this effect can be attributed to the increased level of mixed

326   micelles available to solubilize any lipophilic tangeretin molecules released from the digested

327   zein nanoparticles [25]. At the highest fat content used in this study, the tangeretin concentration in

328   the micelle phase was determined to be 12.4 ± 1.8 μM, while the saturation concentration of

329   tangeretin in pure water is around 0.93 ± 0.02 μM, which clearly shows that the digested lipids

330   were able to greatly increase tangeretin solubilization in the aqueous intestinal fluids.

331   Further information about the properties of the mixed micelle phase was obtained by

332   analyzing the particle size using dynamic light scattering. The mean diameters of the particles in

333   the micelle phase for delivery systems initially containing 0, 2 or 4% oil were 61.5, 69.1 and

12

334   112.5 nm, respectively. In the absence of fat, these particles may have been micelles formed by

335   the bile salts and phospholipids in the simulated small intestinal fluids. In addition, there may

336   have been other forms of particles present in this phase, including protein nanoparticles that were

337   not fully digested. In the presence of fat, the increase in particle size may have been due to the

338   presence of mixed micelles consisting of bile salts, phospholipids, free fatty acids, and

339   monoacylglycerols. The mixed micelle phase resulting from lipid digestion typically contains a

340   combination of small micelles and large vesicle structures [26]. These mixed micelles are able to

341   transfer the lipophilic bioactive components across the mucous layer so that they can be absorbed

342   by epithelium cells [10a, 27].

3.5. Cytotoxicity of tangeretin on Caco-2 cells

344   When performing cell permeability studies it is important to ensure that the material being

345   tested does not appreciably alter cell viability. An MTT assay was therefore carried out to

346   establish the potential toxicity of the mixed micelle phases collected from the simulated GIT on

347   the Caco-2 cell monolayers. Tangeretin dissolved within DMSO did not significantly decrease

348   cell viability over a relatively wide concentration range (**Fig. 6**), *e.g.,* at 0.1 μM almost all the

349   cells were alive, and even at 20 μM the cell viability was still around 80%. Prior to analysis the

350   mixed micelle phases were diluted with buffer solution to obtain a range of tangeretin

351   concentrations. Consequently, both the tangeretin and mixed micelle concentrations in these

352   samples varied. Our results suggest that the mixed micelles had an appreciable impact on cell

353   viability, since when compared at the same tangeretin concentrations they caused more decrease

354   in cell viability than the control (**Fig. 6**). For example, cell viability was close to 100% at 0.1 μM

355   tangeretin (0.1% v/v mixed micelle phase), but only 20% at 20 μM tangeretin (20% v/v mixed

356   micelle phase). This effect may be caused by increased levels of bile salts in the system, since it

357   has previously been reported that these surface active lipids promote cell death by binding to the

358   mitochondrial membrane, which causes loss of cytochrome activity and mitochondrial

359   membrane potential [28]. For this reason, we used a tangeretin concentration of 5 μM in our

360   permeability studies to ensure that the mixed micelles did not promote a significant decline in

361   Caco-2 cell viability.

362   **3.6. Permeability of digested tangeretin micelle on Caco-2 cell monolayer**

363   Tangeretin concentration used for this study was 5 μM based on our MTT result. As shown

364   in **Fig.7a**, Caco-2 cell monolayer integrity was well maintained during the two hour treatment.

365   During The permeability of the Caco-2 cells increased with increasing fat content in the mixed

366   colloidal dispersions, as demonstrated by the faster rate of tangeretin loss from the apical side of

367   the cells for the samples initially containing 4% oil (**Fig. 7b**). In addition, the calculated

368   apparent permeability coefficients (P_{app}) of the tangeretin were $(18.1 \pm 4.5) \times 10^{-6}$, $(17.1 \pm 1.8) \times$

369   10^{-6}, $(19.3 \pm 2.0) \times 10^{-6}$, and $(26.8 \pm 1.8) \times 10^{-6}$ cm/s for the control group, micelles from 0% oil,

370   micelles from 2% oil, and micelles from 4% oil, respectively (**Table 1**). It has been reported that

371   a substance has a high permeability when its P_{app} is greater than 10×10^{-6} cm/s [6], and so all the

372   samples analyzed in this study had high permeability. Nevertheless, the permeability of

373   tangeretin did increase with increasing oil content in the initial delivery system, which can be

374   partly attributed to the ability of the mixed micelles formed by lipid digestion products to

375   increase the intestinal solubility of tangeretin [10a, 10c]. In addition, free fatty acids and emulsifiers

376   are known to enhance intestinal permeability by increasing the dimensions of the tight junctions

377   between epithelium cells [29].

378   **4. Conclusions**

379   This study shows that the bioavailability of tangeretin encapsulated within zein

380   nanoparticles can be increased by mixing them with lipid nanoparticles. This result supports the

381   notion that mixed delivery systems containing combinations of different kinds of nanoparticles

382   may have advantages over single-nanoparticle systems. One kind of nanoparticle may be

383   designed to encapsulate and protect the bioactive agent in a product during storage, whereas the

384   other kind of nanoparticle is designed to increase its bioavailability within the gastrointestinal

385   tract.

386   Light scattering and microscopy measurements showed that mixed colloidal delivery

387   systems could be successfully prepared containing a combination of tangeretin-loaded zein

388   nanoparticles and lipid nanoparticles. These systems appeared to be stable to aggregation and

389   gravitational separation due to their high particle charge and small particle size. When these

390   mixed colloidal delivery systems were passed through a simulated GIT the protein nanoparticles

391 are digested by proteases thereby releasing the tangeretin molecules, whereas the lipid

392 nanoparticles are digested by pancreatic lipases thereby forming mixed micelles. In the absence

393 of lipid digestion products, some of the tangeretin molecules would have been solubilized in

394 simple micelles formed by bile salts and phospholipids, whereas the rest may have formed

395 crystals that remained in the insoluble matter. Conversely, in the presence of lipid digestion

396 products (free fatty acids and monoacylglycerols) the solubilization capacity of the small

397 intestinal fluids for the tangeretin molecules is increased. The absorption of the tangeretin by

398 Caco-2 monolayers also increased in the presence of lipid nanoparticles, which was attributed to

399 a higher level of tangeretin in the micelle phase, and a possible increase in cell permeability.

400 The results of this study have important implications for the design and fabrication of colloidal

401 delivery systems to increase the bioavailability of hydrophobic nutraceuticals and

402 pharmaceuticals.

Acknowledgements

411

References

413 1.   Xiao, H.; Yang, C. S.; Li, S.; Jin, H.; Ho, C.-T.; Patel, T., Monodemethylated polymethoxyflavones from
414 sweet orange (Citrus sinensis) peel Inhibit growth of human lung cancer cells by apoptosis. *Molecular*
415 *Nutrition & Food Research* **2009,** *53* (3), 398-406.

416 2.   Singh, S. P.; Wahajuddin; Tewari, D.; Patel, K.; Jain, G. K., Permeability determination and
417 pharmacokinetic study of nobiletin in rat plasma and brain by validated high-performance liquid
418 chromatography method. *Fitoterapia* **2011,** *82* (8), 1206-1214.

15

419   3.   Kurowska, E. M.; Manthey, J. A., Hypolipidemic Effects and Absorption of Citrus Polymethoxylated
420   Flavones in Hamsters with Diet-Induced Hypercholesterolemia. *J Agr Food Chem* **2004,** *52* (10), 2879-
421   2886.

422   4.   (a) Qiu, P.; Dong, P.; Guan, H.; Li, S.; Ho, C.-T.; Pan, M.-H.; McClements, D. J.; Xiao, H., Inhibitory
423   effects of 5-hydroxy polymethoxyflavones on colon cancer cells. *Molecular Nutrition & Food Research*
424   **2010,** *54* (S2), S244-S252; (b) Pan, M.-H.; Lai, Y.-S.; Lai, C.-S.; Wang, Y.-J.; Li, S.; Lo, C.-Y.; Dushenkov, S.;
425   Ho, C.-T., 5-Hydroxy-3,6,7,8,3',4'-hexamethoxyflavone Induces Apoptosis through Reactive Oxygen
426   Species Production, Growth Arrest and DNA Damage-Inducible Gene 153 Expression, and Caspase
427   Activation in Human Leukemia Cells. *J Agr Food Chem* **2007,** *55* (13), 5081-5091; (c) Sergeev, I. N.; Li, S.;
428   Colby, J.; Ho, C.-T.; Dushenkov, S., Polymethoxylated flavones induce Ca2+-mediated apoptosis in breast
429   cancer cells. *Life Sciences* **2006,** *80* (3), 245-253.

430   5.   Green, C. O.; Wheatley, A. O.; McGrowder, D. A.; Dilworth, L. L.; Asemota, H. N., Citrus peel
431   polymethoxylated flavones extract modulates liver and heart function parameters in diet induced
432   hypercholesterolemic rats. *Food and Chemical Toxicology* **2013,** *51* (0), 306-309.

433   6.   Li, S.; Pan, M.-H.; Lo, C.-Y.; Tan, D.; Wang, Y.; Shahidi, F.; Ho, C.-T., Chemistry and health effects of
434   polymethoxyflavones and hydroxylated polymethoxyflavones. *Journal of Functional Foods* **2009,** *1* (1), 2-
435   12.

436   7.   Chen, J.; Zheng, J.; McClements, D. J.; Xiao, H., Tangeretin-loaded protein nanoparticles fabricated
437   from zein/β-lactoglobulin: Preparation, characterization, and functional performance. *Food Chemistry*
438   **2014,** *158* (0), 466-472.

439   8.   Joye, I. J.; McClements, D. J., Production of nanoparticles by anti-solvent precipitation for use in
440   food systems. *Trends in Food Science & Technology* **2013,** *34* (2), 109-123.

441   9.   (a) Quispe-Condori, S.; Saldaña, M. D. A.; Temelli, F., Microencapsulation of flax oil with zein using
442   spray and freeze drying. *LWT - Food Science and Technology* **2011,** *44* (9), 1880-1887; (b) Wu, Y.; Luo, Y.;
443   Wang, Q., Antioxidant and antimicrobial properties of essential oils encapsulated in zein nanoparticles
444   prepared by liquid–liquid dispersion method. *LWT - Food Science and Technology* **2012,** *48* (2), 283-290;
445   (c) Zhong, Q.; Jin, M., Zein nanoparticles produced by liquid–liquid dispersion. *Food Hydrocolloids* **2009,**
446   *23* (8), 2380-2387.

447   10.   (a) Porter, C. J.; Trevaskis, N. L.; Charman, W. N., Lipids and lipid-based formulations: optimizing the
448   oral delivery of lipophilic drugs. *Nat Rev Drug Discov* **2007,** *6* (3), 231-48; (b) McClements, D. J.; Xiao, H.,
449   Excipient foods: designing food matrices that improve the oral bioavailability of pharmaceuticals and
450   nutraceuticals. *Food & Function* **2014,** *5* (7), 1320-1333; (c) McClements, D. J., Utilizing food effects to
451   overcome challenges in delivery of lipophilic bioactives: structural design of medical and functional
452   foods. *Expert Opinion on Drug Delivery* **2013,** *10* (12), 1621-1632.

453   11.   Ting, Y.; Chiou, Y.-S.; Pan, M.-H.; Ho, C.-T.; Huang, Q., In vitro and in vivo anti-cancer activity of
454   tangeretin against colorectal cancer was enhanced by emulsion-based delivery system. *Journal of*
455   *Functional Foods* **2015,** *15*, 264-273.

456   12.   Ting, Y.; Jiang, Y.; Lan, Y.; Xia, C.; Lin, Z.; Rogers, M. A.; Huang, Q., Viscoelastic Emulsion Improved
457   the Bioaccessibility and Oral Bioavailability of Crystalline Compound: A Mechanistic Study Using in Vitro
458   and in Vivo Models. *Molecular Pharmaceutics* **2015,** *12* (7), 2229-2236.

459   13.   Parris, N.; Cooke Peter, H.; Moreau Robert, A.; Hicks Kevin, B., Encapsulation of Essential Oils in Zein
460   Nanospherical Particles. In *New Delivery Systems for Controlled Drug Release from Naturally Occurring*
461   *Materials*, American Chemical Society: 2008; Vol. 992, pp 175-192.

462   14.   Christensen, J. Ø.; Schultz, K.; Mollgaard, B.; Kristensen, H. G.; Mullertz, A., Solubilisation of poorly
463   water-soluble drugs during in vitro lipolysis of medium- and long-chain triacylglycerols. *European Journal*
464   *of Pharmaceutical Sciences* **2004,** *23* (3), 287-296.

465   15.   Li, Y.; McClements, D. J., Controlling lipid digestion by encapsulation of protein-stabilized lipid
466   droplets within alginate–chitosan complex coacervates. *Food Hydrocolloids* **2011,** *25* (5), 1025-1033.

467   16.   Sarkar, A.; Goh, K. K. T.; Singh, H., Colloidal stability and interactions of milk-protein-stabilized
468   emulsions in an artificial saliva. *Food Hydrocolloids* **2009,** *23* (5), 1270-1278.

469   17.   Li, Y.; McClements, D. J., New Mathematical Model for Interpreting pH-Stat Digestion Profiles:
470   Impact of Lipid Droplet Characteristics on in Vitro Digestibility. *J Agr Food Chem* **2010,** *58* (13), 8085-
471   8092.

472   18.   Dong, P.; Qiu, P.; Zhu, Y.; Li, S.; Ho, C.-T.; McClements, D. J.; Xiao, H., Simultaneous determination of
473   four 5-hydroxy polymethoxyflavones by reversed-phase high performance liquid chromatography with
474   electrochemical detection. *Journal of Chromatography A* **2010,** *1217* (5), 642-647.

475   19.   Horie, M.; Kato, H.; Fujita, K.; Endoh, S.; Iwahashi, H., In Vitro Evaluation of Cellular Response
476   Induced by Manufactured Nanoparticles. *Chemical Research in Toxicology* **2011,** *25* (3), 605-619.

477   20.   Ina, H.; Eva, G. E. R.; Per, A., Determination of drug permeability and prediction of drug absorption
478   in Caco-2 monolayers. *Nature Protocols* **2007,** *2* (9), 2111-2119.

479   21.   McClements, D. J., Crystals and crystallization in oil-in-water emulsions: Implications for emulsion-
480   based delivery systems. *Advances in Colloid and Interface Science* **2012,** *174*, 1-30.

481   22.   Vingerhoeds, M. H.; Blijdenstein, T. B. J.; Zoet, F. D.; van Aken, G. A., Emulsion flocculation induced
482   by saliva and mucin. *Food Hydrocolloids* **2005,** *19* (5), 915-922.

483   23.   Cuyckens, F.; Claeys, M., Mass spectrometry in the structural analysis of flavonoids. *Journal of Mass*
484   *Spectrometry* **2004,** *39* (1), 1-15.

485   24.   McClements, D. J.; Li, F.; Xiao, H., The Nutraceutical Bioavailability Classification Scheme: Classifying
486   Nutraceuticals According to Factors Limiting their Oral Bioavailability. *Annual review of food science and*
487   *technology* **2015,** *6*, 299-327.

488   25.   Thakkar, S. K.; Maziya-Dixon, B.; Dixon, A. G.; Failla, M. L., Beta-carotene micellarization during in
489   vitro digestion and uptake by Caco-2 cells is directly proportional to beta-carotene content in different
490   genotypes of cassava. *J Nutr* **2007,** *137* (10), 2229-33.

491   26.   Phan, S.; Salentinig, S.; Gilbert, E.; Darwish, T. A.; Hawley, A.; Nixon-Luke, R.; Bryant, G.; Boyd, B. J.,
492   Disposition and crystallization of saturated fatty acid in mixed micelles of relevance to lipid digestion.
493   *Journal of Colloid and Interface Science* **2015,** *449*, 160-166.

494   27.   Lafitte, G.; Thuresson, K.; Soderman, O., Diffusion of nutrients molecules and model drug carriers
495   through mucin layer investigated by magnetic resonance imaging with chemical shift resolution. *Journal*
496   *of Pharmaceutical Sciences* **2007,** *96* (2), 258-263.

497   28.   Schulz, S.; Schmitt, S.; Wimmer, R.; Aichler, M.; Eisenhofer, S.; Lichtmannegger, J.; Eberhagen, C.;
498   Artmann, R.; Tookos, F.; Walch, A.; Krappmann, D.; Brenner, C.; Rust, C.; Zischka, H., Progressive stages
499   of mitochondrial destruction caused by cell toxic bile salts. *Biochimica et Biophysica Acta (BBA) -*
500   *Biomembranes* **2013,** *1828* (9), 2121-2133.

501   29.   Ulluwishewa, D.; Anderson, R. C.; McNabb, W. C.; Moughan, P. J.; Wells, J. M.; Roy, N. C.,
502   Regulation of tight junction permeability by intestinal bacteria and dietary components. *J Nutr* **2011,** *141*
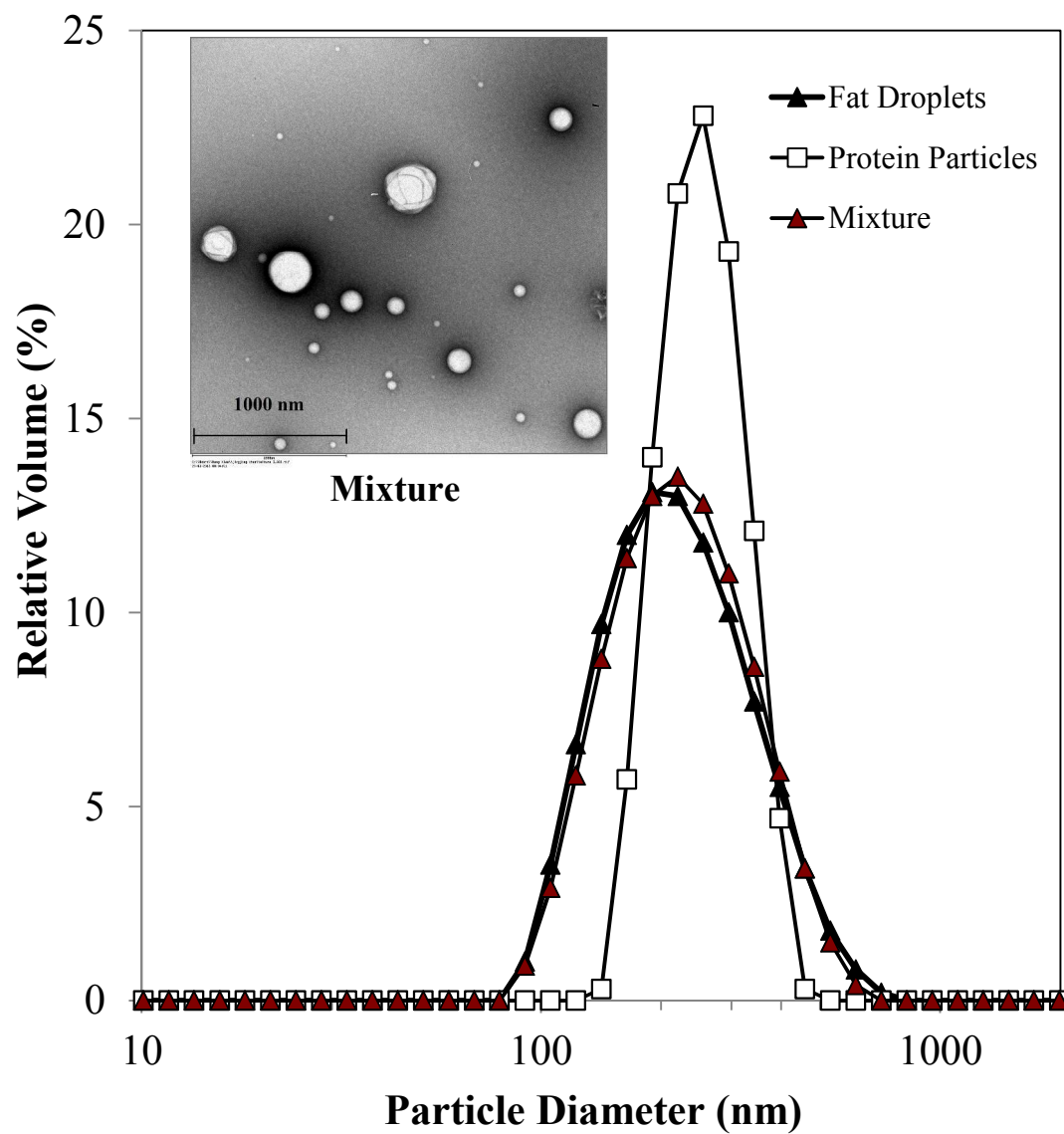503   (5), 769-76.
504
505

Figure 1. Particle size distribution of fat droplets, protein nanoparticles, and the mixed system.

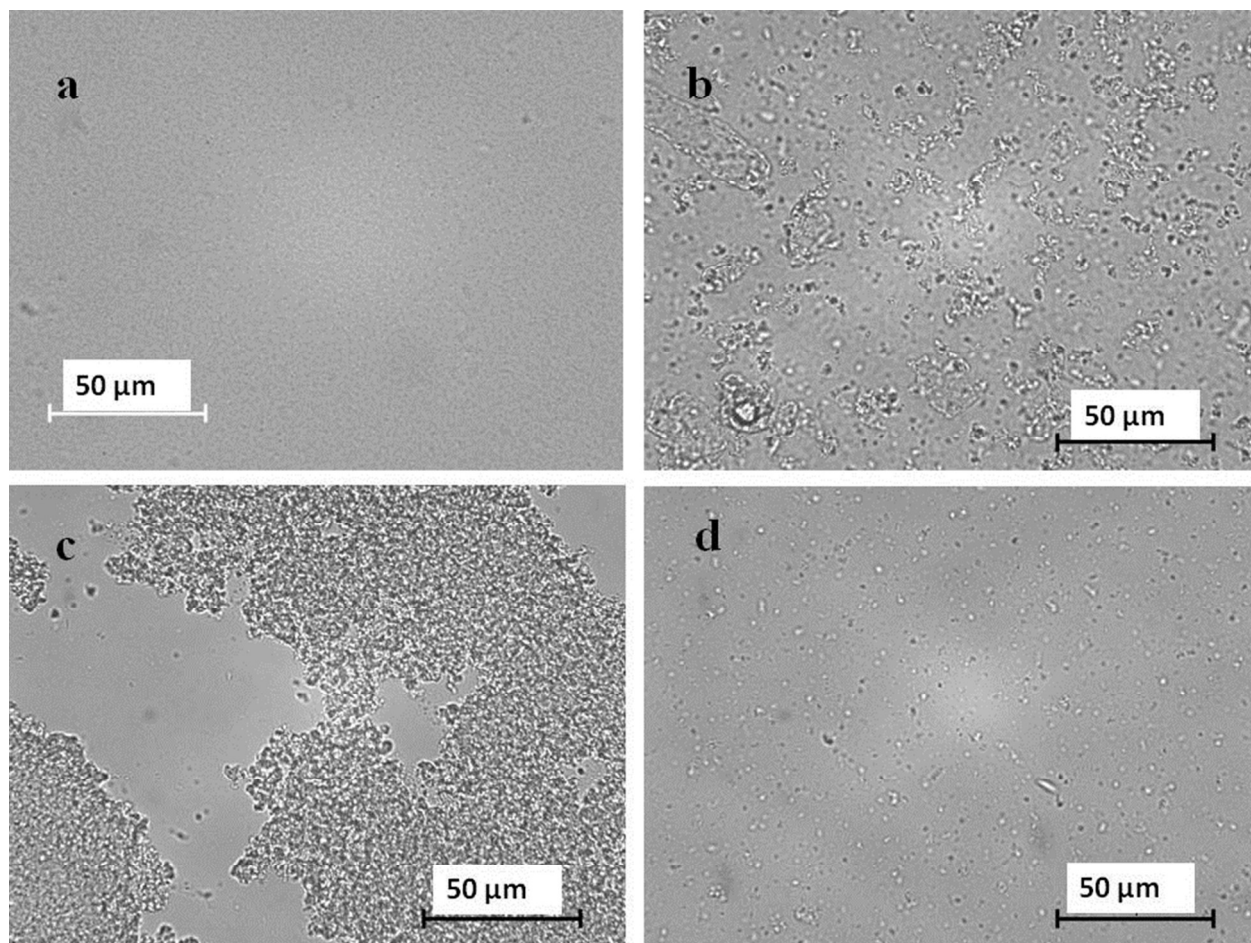The inset shows a transmission electron microscopy image of the mixed system.

Figure 2. Microscopic image of initial delivery system (a) and delivery system after digestion in

(b) mouth, (c) stomach, (d) small intestine.
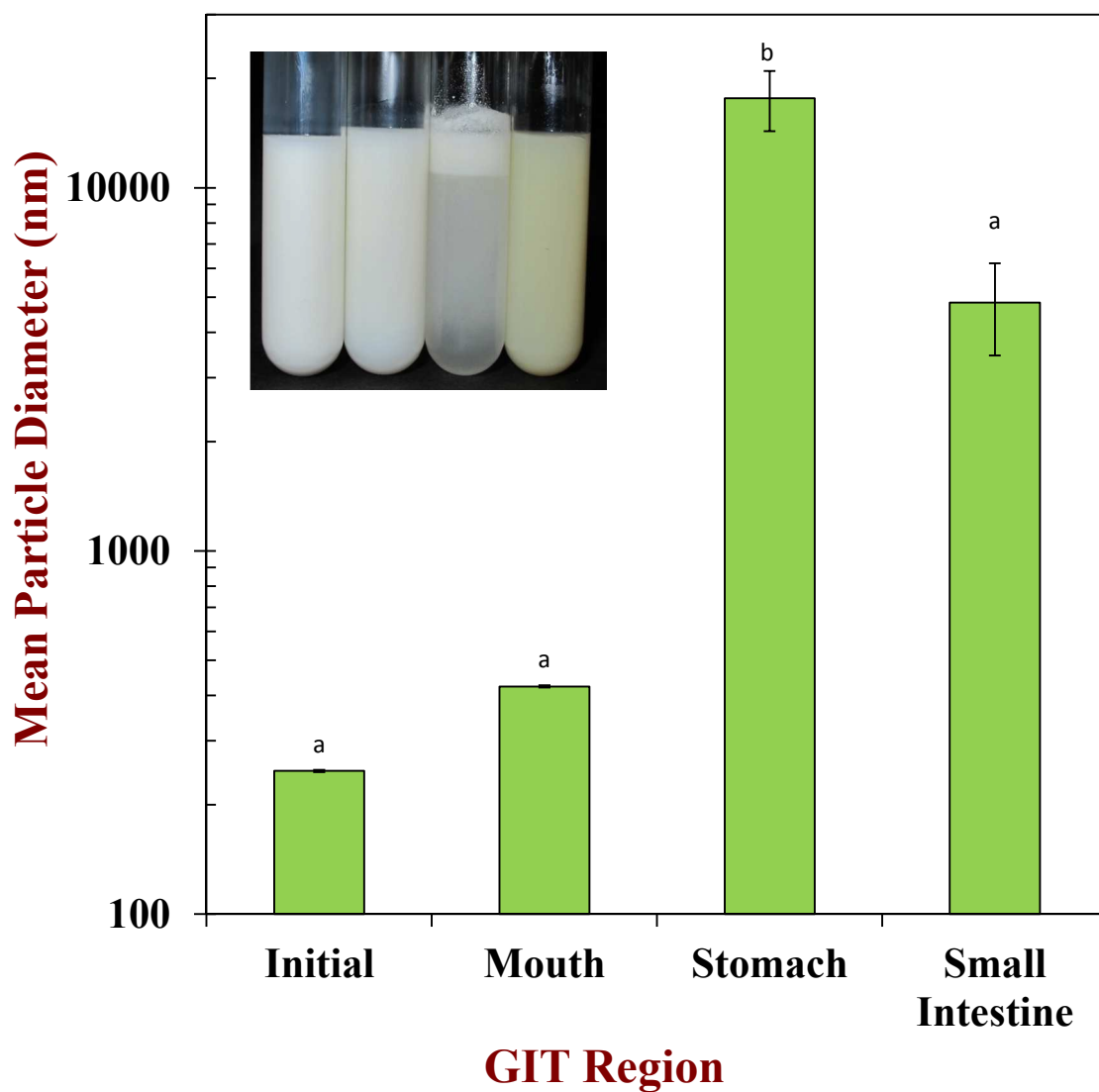
Figure 3a. Mean particle diameters and appearances of mixed systems initially containing

protein nanoparticles and lipid nanoparticles (2% oil) after passage through various stages of a

simulated gastrointestinal tract (GIT). The inset shows the appearance of the system at different

digestion stages (Means with different letters are significantly different, p<0.05).
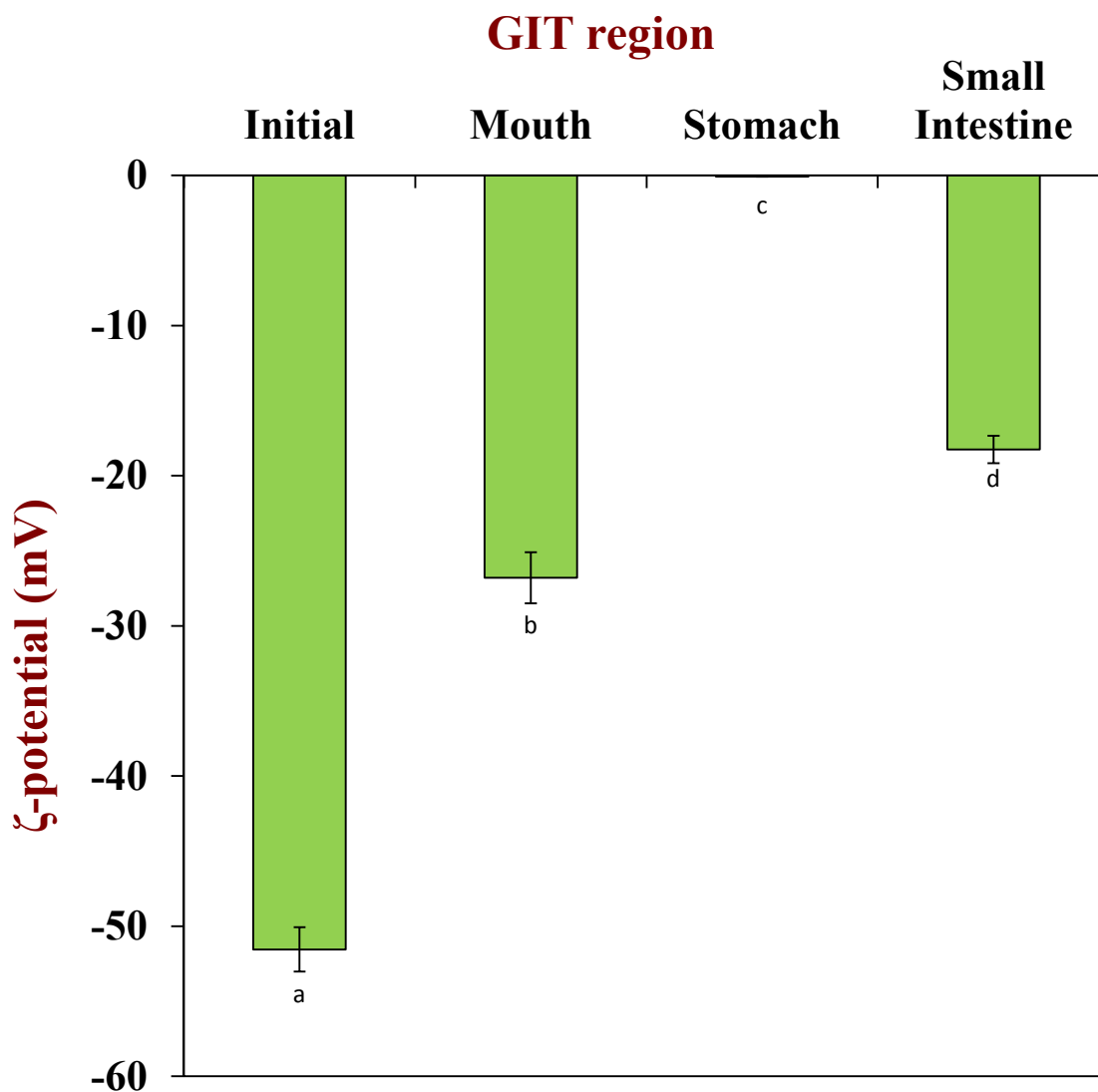
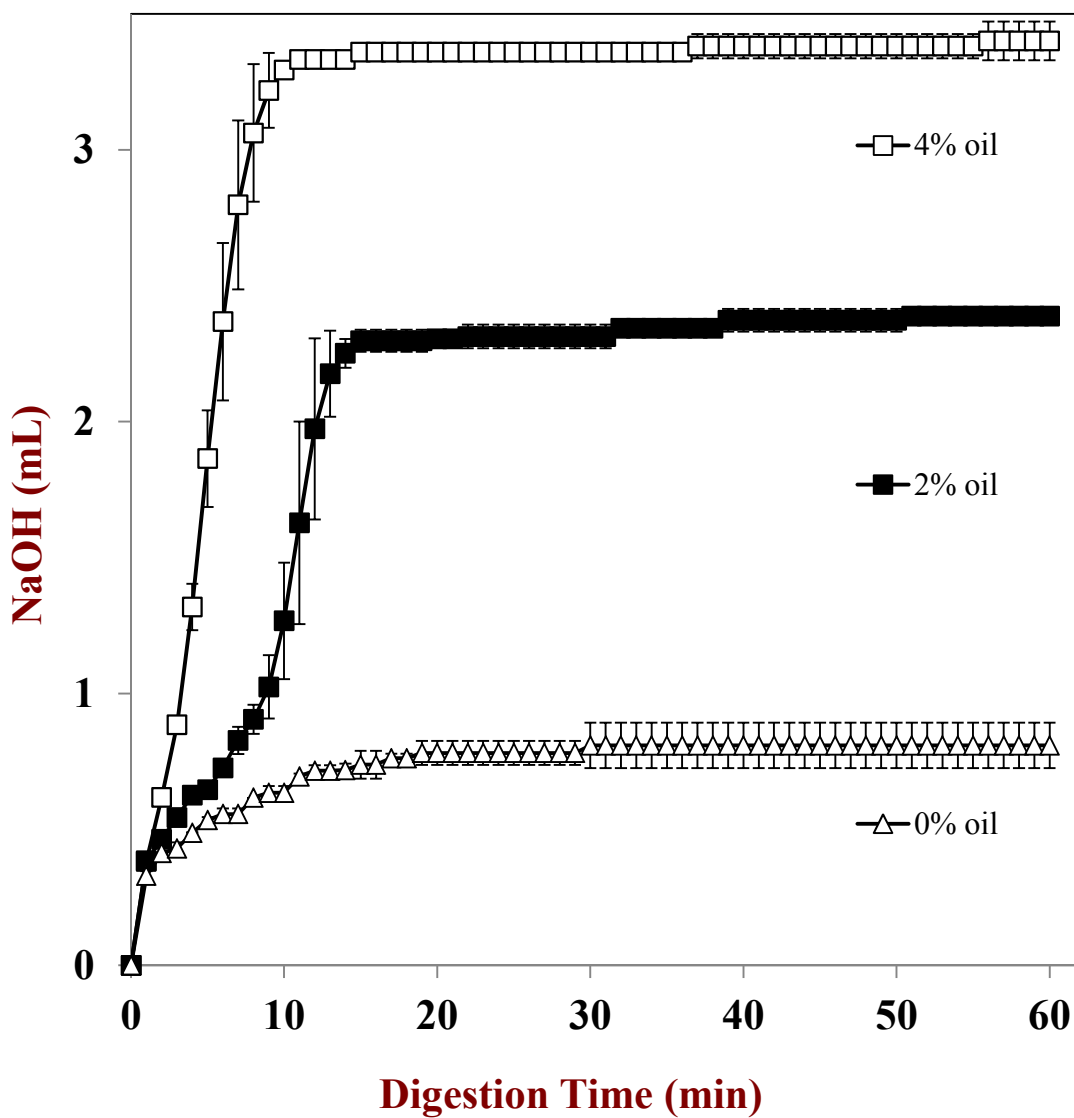**Figure 3b**. Mean particle charges of mixed systems initially containing protein nanoparticles and lipid nanoparticles (2% oil) after passage through various stages of a simulated gastrointestinal tract (GIT). The inset shows the appearance of the system at different digestion stages. (Means with different letters are significantly different, $p<0.05$).

Figure 4a. pH-Stat titration curves carried out under simulated small intestinal conditions for mixed colloidal delivery systems containing tangeretin-loaded zein nanoparticles and different concentrations of lipid nanoparticles (0 to 4% oil).
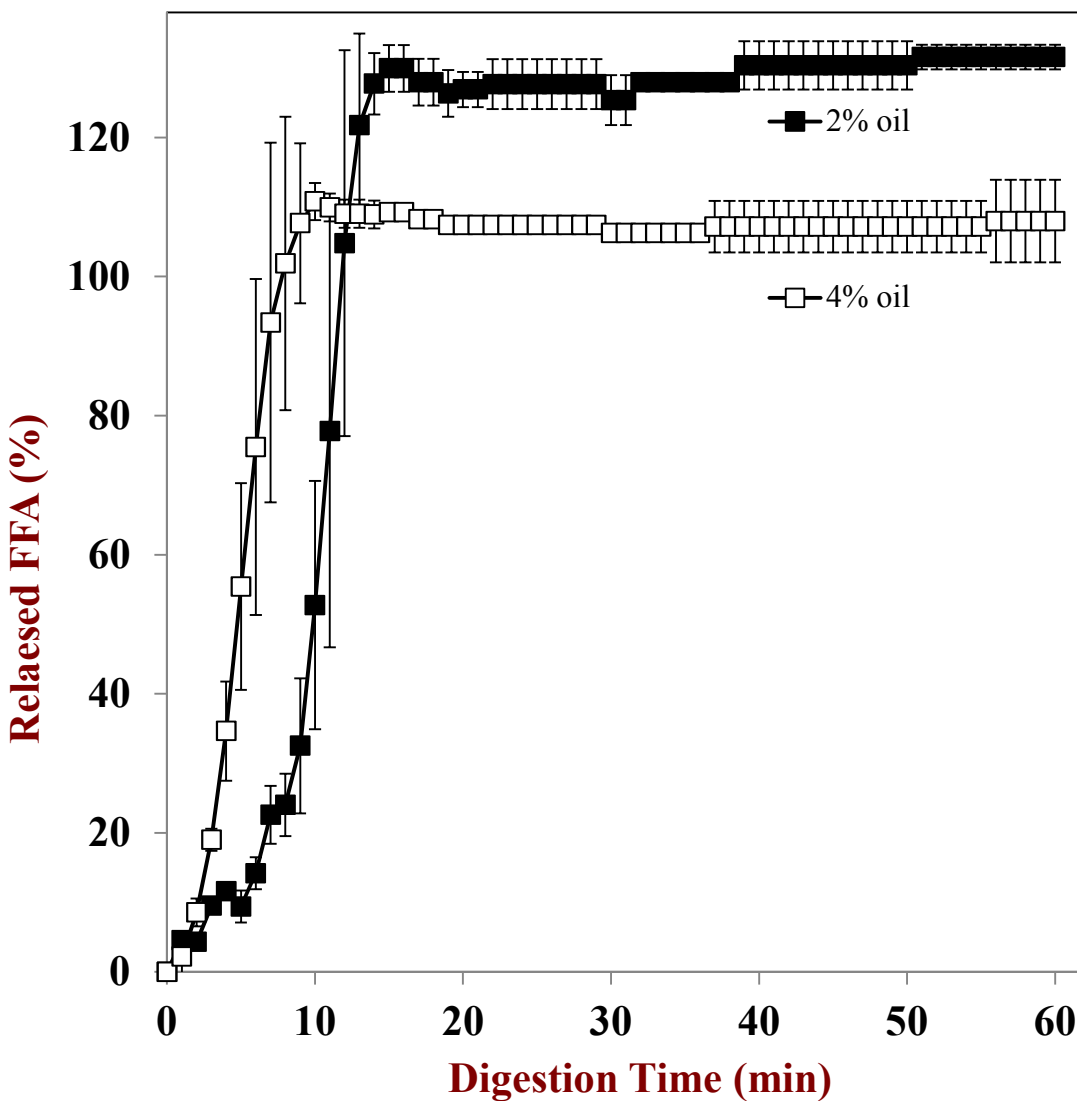
Figure 4b. Calculated free fatty acids released under simulated small intestinal conditions for

mixed colloidal delivery systems containing tangeretin-loaded zein nanoparticles and different

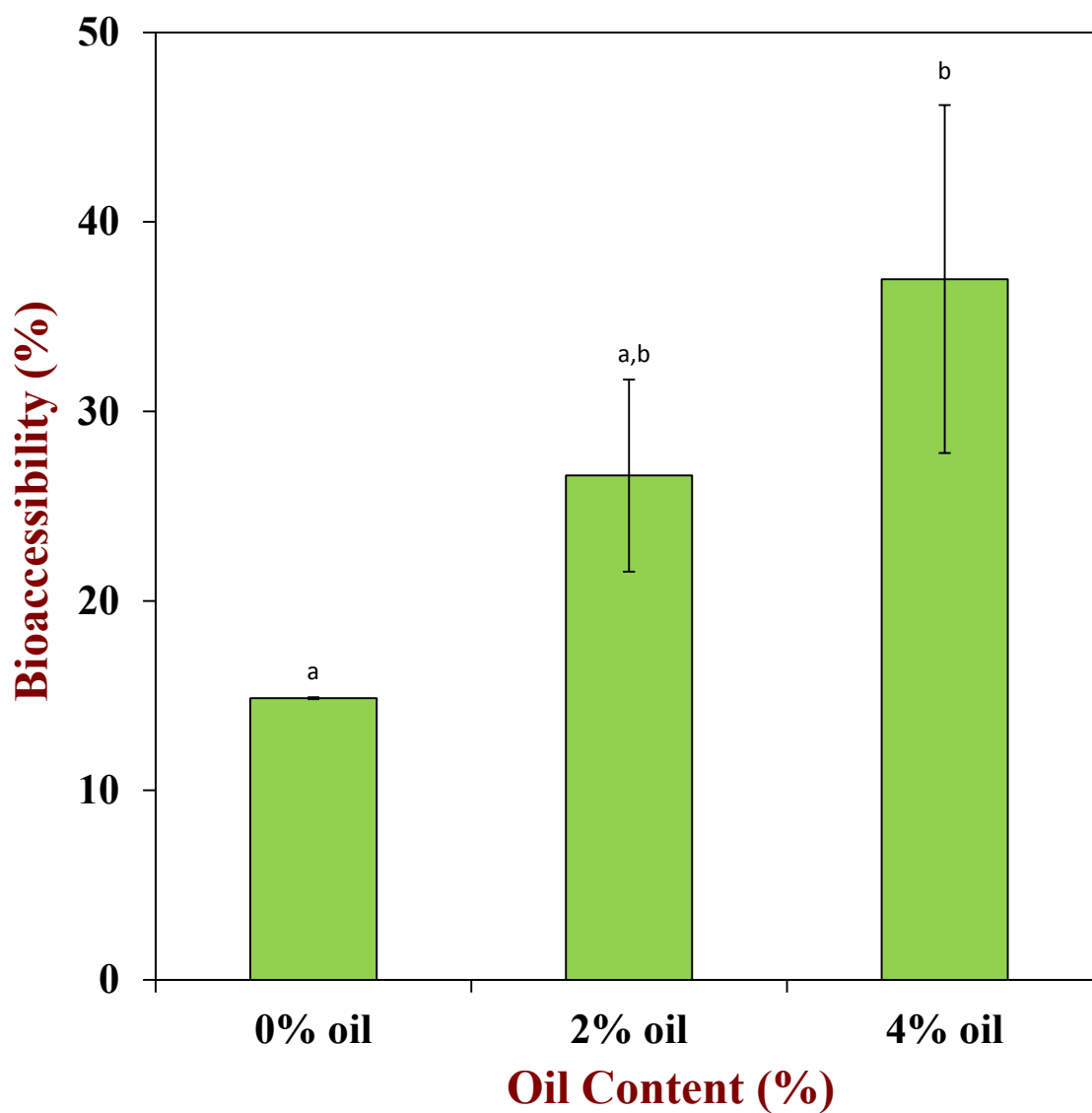initial concentrations of lipid nanoparticles (2 or 4% oil).

Figure 5. Influence of initial oil content on tangeretin bioaccessibility in mixed colloidal

delivery systems containing tangeretin-loaded zein nanoparticles and lipid nanoparticles (Means

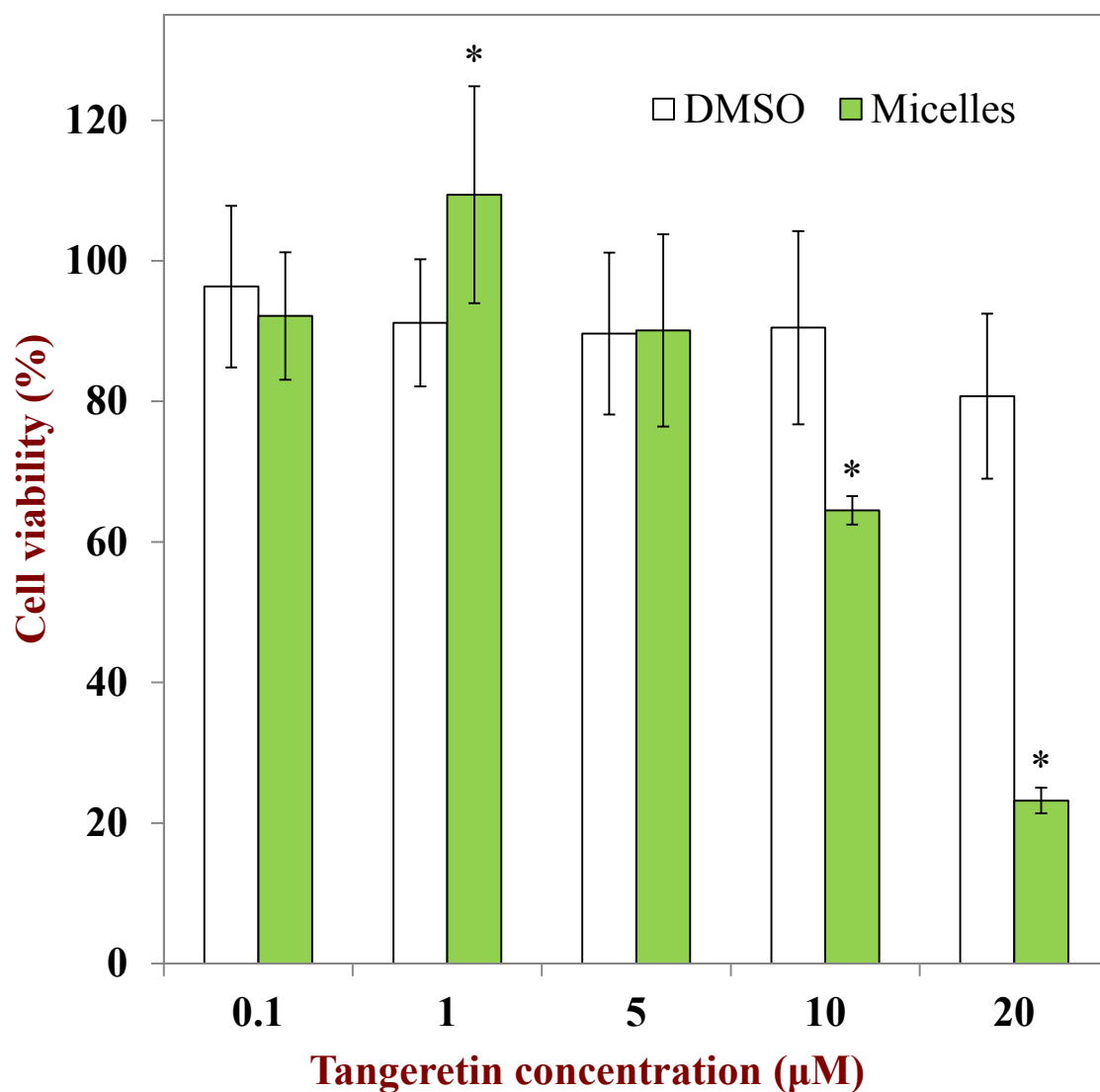with different letters are significantly different, $p<0.05$).

Figure 6. Influence of tangeretin dissolved in DMSO or mixed micelles on Caco-2 cell viability. Cells were seeded at 20,000 cells/well on a 96 well plate 24 hours before treatment. The samples were diluted using serum complete media to obtain a range of tangeretin concentrations (*, $p < 0.05$).
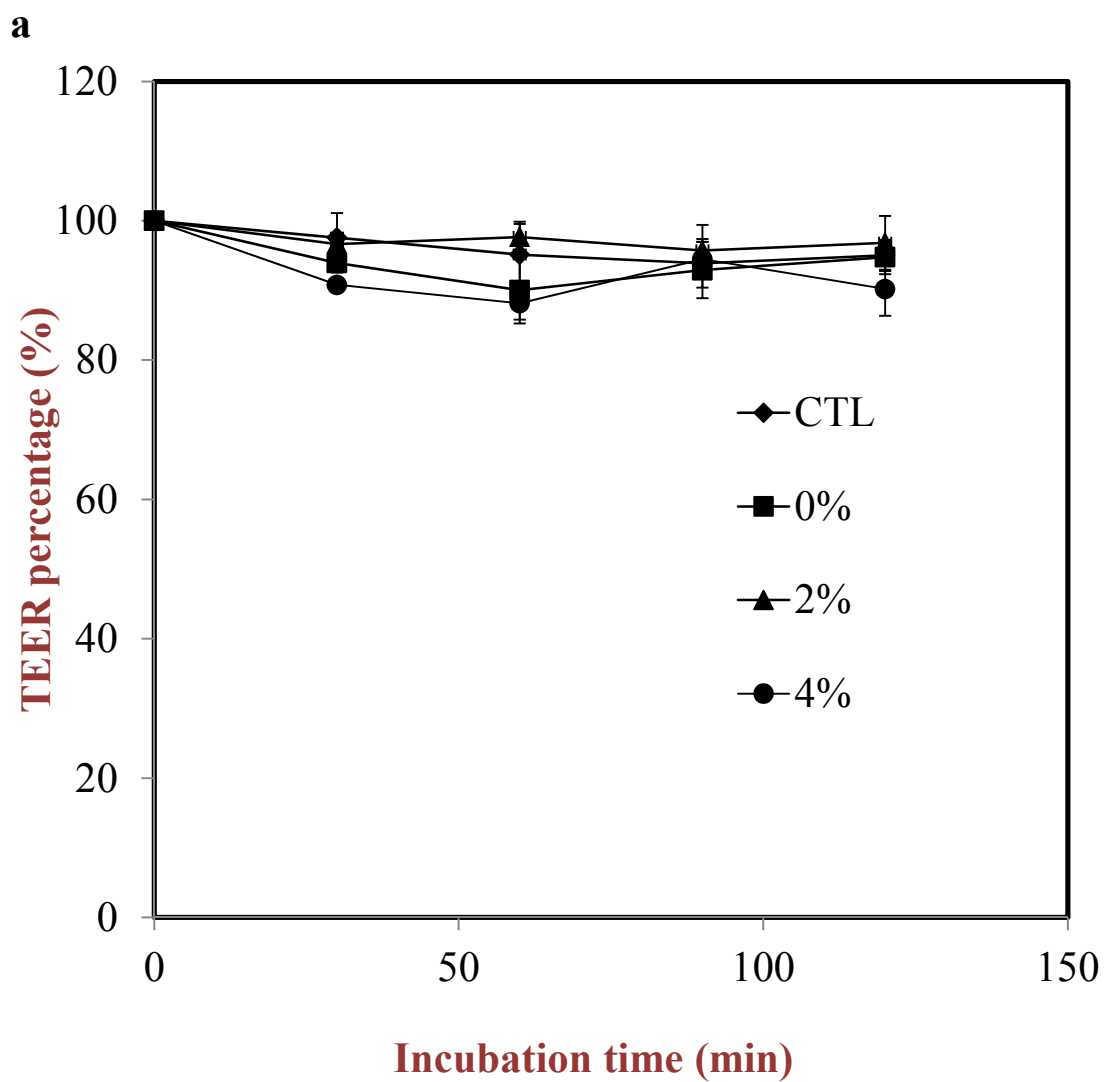
a

Figure 7a. TEER percentage of each sample at different time.
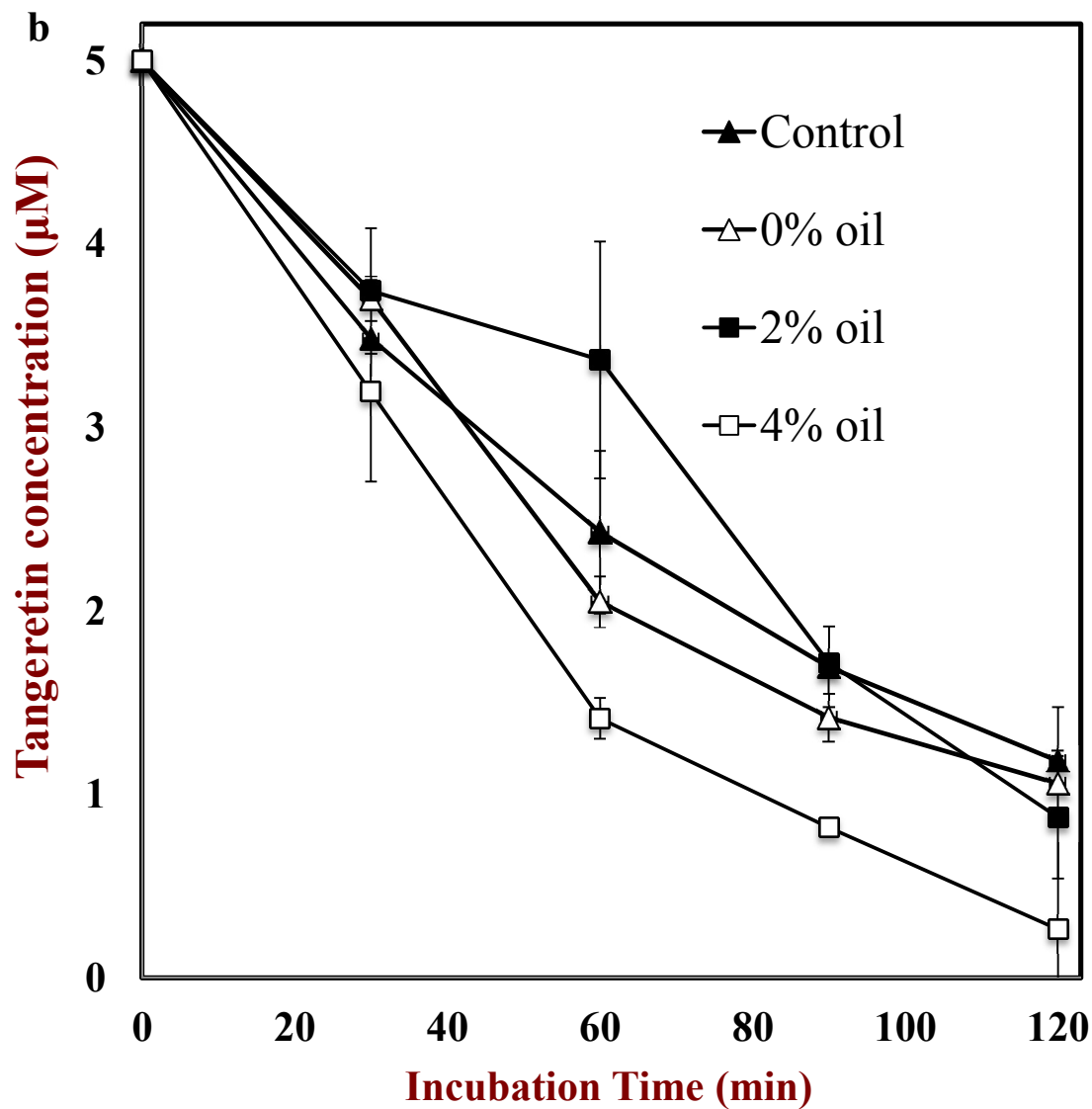
b

Figure 7b: Tangeretin concentration in the apical compartment of Caco-2 transwell cells at different times for different delivery systems. *Control*: tangeretin dissolved in HBSS; 0% oil: digested phase from tangeretin nanoparticles with no oil; 2%: digested phase from tangeretin nanoparticles mixed with 2% oil; 4%: digested phase from tangeretin nanoparticles mixed with 4% oil. The oil was delivered as lipid nanoparticles.

Table 1. Caco-2 monolayer permeability of digested phases from delivery systems initially

containing tangeretin nanoparticles and different oil contents (delivered in the form of lipid

nanoparticles). The control consisted of tangeretin dissolved in DMSO.

Delivery System	P_{app} ($\times 10^{-6}$ cm/s)
Control	18.1 ± 4.5^a
0% oil	17.1 ± 1.8^a
2% oil	19.3 ± 2.0^a
4% oil	26.8 ± 1.8^b

*Means with different letters are significantly different, $p<0.05$.